

RSC Advances



This is an *Accepted Manuscript*, which has been through the Royal Society of Chemistry peer review process and has been accepted for publication.

Accepted Manuscripts are published online shortly after acceptance, before technical editing, formatting and proof reading. Using this free service, authors can make their results available to the community, in citable form, before we publish the edited article. This *Accepted Manuscript* will be replaced by the edited, formatted and paginated article as soon as this is available.

You can find more information about *Accepted Manuscripts* in the [Information for Authors](#).

Please note that technical editing may introduce minor changes to the text and/or graphics, which may alter content. The journal's standard [Terms & Conditions](#) and the [Ethical guidelines](#) still apply. In no event shall the Royal Society of Chemistry be held responsible for any errors or omissions in this *Accepted Manuscript* or any consequences arising from the use of any information it contains.

Density functional studies of small silicon clusters adsorbed on graphene

Yongliang Yong^{1, 2,*}, Xiping Hao¹, Chao Li¹, Xiaohong Li¹, Tongwei Li¹, Hongling Cui¹ and Shijie Lv¹

¹ College of Physics and Engineering, Henan University of Science and Technology, Luoyang 471003, People's Republic of China

² Department of Physics, Zhejiang University, Hangzhou 310027, People's Republic of China

ABSTRACT

The structural and electronic properties of small Si_n clusters ($n=1-6, 10$) adsorbed on graphene are studied by use of density functional theory within periodic boundary conditions. Our results show that the structural properties of the deposited Si_n clusters and graphene are weakly affected by their interaction. The adsorption energy difference of different adsorption sites for the same size Si cluster on graphene is very small, indicating the Si_n -cluster/graphene system will be obtained easily. There is a little charge transfer from Si_n clusters to graphene when the cluster size is larger. The adsorption of Si_n clusters will be an effective method to open of an energy gap for graphene, which is useful for the applications of graphene to electrical and optical devices. Especially, the adsorption of Si_n cluster with large size ($n \geq 5$) would have a band gap with a constant energy value.

Keywords: Small silicon clusters, Graphene, Adsorption properties, Density functional theory.

* Author to whom correspondence should be addressed. Electronic mail: ylyong@haust.edu.cn

1. Introduction

The interaction between cluster and surface has been an important concern of experimental and theoretical studies in the past years. The interest, on one hand, is driven by the need to understand the fundamental aspects of the mechanisms involved in the interaction (such as diffusion-limited aggregation [1], fragmentation [2], and self-assembly [3] of clusters on the surface); on the other hand, a deep understanding of the properties of the cluster-surface interaction is of great interest in their technological applications such as nano-electronics [4-6] and (heterogeneous) catalysis [7-9]. Moreover, with the development of efficient *ab initio* methods and increasing computational power, it is more feasible for theoretical investigations of the cluster-surface interaction processes on the atomic scale than previous decades. One crucial aspect of the interactions between cluster and surface is the adsorption on process of clusters, which can be used, for example, to understand (i) how the clusters modify the structural, electronic, and magnetic properties of the substrate surface, which is of relevance to growing thin films; (ii) how the physical and chemical properties of the isolated clusters may be engineered and tuned for potential applications on a surface.

In particular, the interaction of carbonaceous materials such as fullerenes, carbon nanotubes, graphite and graphene with atoms (molecules) and clusters share many peculiar properties. In this work, we are concerned with the interaction between small silicon clusters and graphene. Graphene, since its discovery [10], has attracted numerous experimental and theoretical investigations because of its fundamental significance for physics and chemistry and its potential applications for the next generation electronic devices [11-17]. Graphene is a strictly two-dimensional flat form of carbon with atoms arranged in a honeycomb lattice [18,19], whose

planar geometry consisting of sp^2 -hybridized carbon indicates that it is an ideal surface for studying the adsorption of clusters on surface. Moreover, graphene is a strictly zero band gap semiconductor, and its Fermi level exactly crosses the Dirac point. The absence of a band-gap is one major hindrance for graphene's application in nano-electronic devices. Various mechanisms for opening an energy gap have been developed such as breaking certain symmetries in graphene using interaction with other atoms or molecules [20-24], defects [25], and so on. The interaction between clusters and graphene, should be a feasible way to open an energy gap for graphene. Meanwhile, the interaction will tune and change the other properties of graphene. Noting that the fundamental knowledge of the changes of properties is essential for applications.

There are a few investigations on the interaction between clusters and graphene, mainly focusing on the adsorption properties of metal [26-33] and water [34] clusters on graphene. Particularly, the metal clusters are mainly alkali and transitionmetal clusters. For example, Neek-Amal *et al* [28] have reported a systematic theoretical study of the formation of atomic (Cu, Ag, Au, Li, Na, and K) nanoclusters on suspended graphene sheets using temperature-dependent molecular dynamics simulations at finite temperature. They found that transition metal atoms aggregate and make various size nanoclusters distributed randomly on graphene surfaces, while most alkali atoms make one atomic layer on graphene sheets. Yoo *et al* [29] presented an experimental result for Pt subnanoclusters supported on graphene nanosheet surface (GNS). They have found Pt particles below 0.5 nm in size are formed on GNS, which would acquire the specific electronic structures of Pt, modifying its catalytic activities. Aktürk and Tomak [31] investigated structural, electronic and magnetic properties of Au_nPt_n ($n=1-3$) clusters adsorbed on graphene surface through first-principle calculations based on density functional theory within

localized density approximation and generalized gradient approximation. They observed that graphene can be metallic or semiconducting depending on number of platinum and gold atoms in the clusters. Okazaki-Maeda and co-workers [32] have investigated the stability of Pt_n ($n=1-13$) clusters on a graphene sheet and the interfacial interaction between Pt_n ($n=1-13$) clusters and graphene surface using first-principles calculations based on density functional theory. Meanwhile, Leenaerts and co-workers [34] have examined the adsorption of H_2O on graphene containing up to five water molecules using density functional theory within the generalized gradient approximation of Perdew-Burke-Ernzerhof. They found that graphene is highly hydrophobic and adsorbed water has very little effect on the electronic structure of graphene.

It is noted that the above mentioned investigations on the cluster-graphene interaction have, however, been no concern with the semiconductor clusters. In the past two decades, the semiconductor clusters have been extensively studied based on theoretical and experimental techniques, because of their fundamental role in cluster physics and chemistry as well as their promising potential applications in view of the current miniaturization trends and the existing infrastructure. In particular, silicon clusters have been the focus of numerous theoretical and experimental studies in recent years yielding mainly equilibrium geometries and electronic properties (for example, see Refs. 35-45). It is well known that small silicon clusters formed in free space without any supporting substrates have different lowest-energy structures from the crystalline silicon. Meanwhile silicon clusters show numerous new properties, which are absent in the bulk. For example, photoluminescence is found in small silicon clusters [46]. Little is known about the atomic processes of silicon clusters on graphene, which is very different from the situation on other surfaces because of its two-dimensional structure. We believe that the

interaction between silicon clusters and graphene will affect the properties of the clusters as well as the properties of graphene.

To the best of our knowledge, only Wu *et al* [47, 48] have studied small silicon clusters adsorbed on graphite (0001) and diamond (100) surfaces by density functional theory within periodic boundary conditions, but there is no work on the interactions between small Si_n clusters and graphene surface. In this work, we report the results of density functional calculations for small Si_n ($n=1-6, 10$) clusters adsorbed on graphene. Of particular interest is the effect on each other. The theoretical details and computational methods are described briefly in the next section. Subsequently, we present and discuss the theoretical results. Finally, the general overview and conclusions are given.

2. Computational details

All calculations were performed on Si_n ($n=1-6, 10$) clusters adsorbed on graphene, in the framework of density-functional theory (DFT), using the DMOL³ program (Accelrys Inc.) [49, 50]. The generalized gradients approximation (GGA) for the exchange and correlation in the Perdew-Burke-Ernzerhof form [51] and double numerical basis sets supplemented with d polarization functions (the DNP sets) are chosen for the spin-polarized DFT calculations within periodic boundary conditions. The all electron treatment for core treatment is used to describe all atoms (Si and C) in a given system. Self-consistent-field (SCF) electronic structure calculations were carried out with a convergence criterion of 10^{-6} hartree on the total energy on all systems. Simultaneously, all structures were fully optimized without any symmetry constraint with a convergence criterion of 0.002 hartree/Å for the forces and 0.005 Å for the displacement. It is well known that chemical bonding and electron transfer can be described well within GGA. However,

van der Waals (vdW) forces are not represented well by the GGA functional. In our calculations, we considered vdW interaction between Si_n ($n=1-6, 10$) cluster-adsorbates and graphene using Tkatchenko-Scheffler (TS) methods [52]. The dispersion-corrected DFT (DFT-D) have been widely used to study adsorption of organic molecules on graphene (e.g. refs. 53-56).

The structure of graphene is made out of carbon atoms arranged in hexagonal structure, and it can be regarded as a triangular lattice with a basis of two atoms per unit cell. We use our calculated graphene lattice constant of 2.46 Å, which is the same as the experimental value. The calculated cluster-graphene system model used here consists of a 4×4 graphene supercell (32 C atoms) to investigate the interaction of Si_n clusters adsorbed at different sites on the surface, which corresponds to a coverage of one silicon cluster per 32 C atoms and the in-plane lattice constant is 9.84 Å. In order to ensure the 4×4 graphene supercell is appropriate for all simulations, several test calculations for 98-atom graphene (7×7 supercell) gave essentially the same results, which indicate the 4×4 graphene supercell is adequate. For the largest size cluster Si_{10} we considered, there is still a distance of at least 6.3 Å between the neighboring Si_{10} clusters, while for the small size clusters the distance is bigger between the neighboring clusters. This indicates that the cluster-cluster interaction is weak enough that can be negligible. The supercells are constructed with a 15 Å vacuum gap normal to the graphene sheet in order to avoid the interaction between graphene layers of adjacent supercells. For full relaxation of all systems and electronic properties calculations, the Monkhorst-Pack k-point mesh of 5×5×1 (Γ point included) was used for Brillouin zone integration [57]. Meanwhile tests using 9×9×1 k-points for full relaxation of all systems and electronic properties calculations got the same results.

In our investigations of Si_n ($n=1-6, 10$) clusters adsorbed on the graphene surface, we roughly

study in the following steps: Firstly, we obtain the lowest-energy structures of Si_n ($n=1-6, 10$) clusters in an aperiodic environment using the same methods as above mentioned. Secondly, the Si_n clusters/graphene system is fully relaxed to equilibrium geometries using DFT-D. The cluster was initially located about 2 Å above the graphene by taking into account the various sites, either paralleling or perpendicular to graphene surface. It is noted that no constraints were performed upon the geometric configurations of Si_n clusters, graphene, or cluster-graphene system. Finally, the most stable cluster-graphene systems are found to research their properties. Calculations for the pristine 4×4 graphene and 4×4 cluster-graphene system are performed with the same-sized hexagonal supercell. To calculate adsorption energies, we also require the total energy of an isolated Si_n cluster, which is obtained by calculating the isolated Si_n cluster in a hexagonal supercell of dimension 9.84 × 9.84 × 15.00 Å³ and the same k-points of the Brillouin zone as the above mentioned is sampled in the case.

The linear or quadratic synchronous transit (LST/QST) transition state (TS) search algorithm combined with conjugate gradient refinements and TS optimization techniques are used to construct a reaction pathway and explore the energy barriers of the structural evolution processes [58]. A vibrational analysis is carried out to confirm that the transition state configuration is stationary after a successful TS search calculation. A true transition state will have exactly one mode with a negative vibrational frequency (imaginary vibrational), while all other frequencies will be real. Meanwhile, the confirmation calculations with the nudged-elastic band (NEB) algorithm [59] are performed to ensure the direct connection of transition states with the respective reactant and product.

3. Results and discussion

Before discussing the small Si_n clusters adsorbed on graphene, we first examined the properties of the pure Si_n ($n=1-6, 10$) cluster-adsorbates and pure graphene substrate. We have investigated the geometry and stability of Si_n ($n=1-6, 10$) clusters using density functional theory with the GGA-PBE functionals. In this work, we mainly use the lowest-energy structures of Si_n ($n=1-6, 10$) clusters as the adsorbates, which are shown in Fig. 1. To obtain the lowest-energy structures of Si_n ($n=1-6, 10$) clusters, we consider as many initial chemical configurations as possible, which are set up by random selections of atomic positions in three dimensional space. In addition, we also considered the configurations, which are mentioned in previous reports [35, 37, 40, 41]. We found that our results for the structural and electronic properties of Si_n ($n=1-6, 10$) clusters are coincident with the previous reports (e.g. refs. 37, 40, 41). Since the structural and electronic properties of small silicon clusters have been intensively studied, here we just give the structures of Si_n ($n=1-6, 10$) clusters, and do not discuss their structural and electronic properties in detail. Meanwhile, we found that the dispersion forces do not affect the structural and electronic properties of Si_n ($n=1-6, 10$) clusters. On the other side, the properties of pure graphene are also calculated to test and ensure the equitable of the models.

The relative stabilities of the cluster-graphene systems are determined by the adsorption energies. It is well-known that the larger the adsorption energy, the binding of the adsorbate to graphene surface is stronger. The adsorption energy, in this work, is defined as

$$E_a = E_{cg} - E_c - E_g \quad (1)$$

where E_{cg} is the total energy of the optimized cluster-graphene system, E_c is the total energy of the isolated Si_n cluster, and E_g is the total energy of the isolated graphene per 4×4 supercell. In order to describe the vdW interaction between graphene and Si_n cluster, here all the total energies are

calculated using DFT-D methods. It should be noted that the adsorption energies, which we would discuss in the following work, are the energies with considering the vdW interaction.

We calculated the cluster-graphene distance (H) to describe the cluster locations on graphene surface after equilibrium geometries. For notation, in our calculated model, we define that the x and y directions be parallel and the z direction be perpendicular to the graphene plane. With the notation, we define the cluster-graphene distance (H) as the difference in the average of the z coordinates of the C atoms in the graphene layer and the z coordinate of the nearest Si atoms in Si_n cluster. Moreover, we also calculated the nearest-neighbor Si-C distance ($D_{\text{Si-C}}$) between Si_n cluster and graphene surface. Adsorption energies and structural properties for the lowest-energy structures of cluster-graphene systems are summarized in [Table 1](#) and [Fig. 2-8](#).

In this work, we consider as many sites as possible for each Si_n cluster adsorbed on graphene, in order to obtain the lowest-energy structures of cluster-graphene systems. Then we will focus on Si_n ($n=1-6, 10$) cluster-adsorbates adsorbed on graphene.

3.1 Structural properties of Si_n ($n=1-6, 10$) clusters adsorbed on graphene

First of all, we examined the single silicon atom adsorption on graphene. We considered three adsorption sites for the silicon atom on graphene surface, which are the top site above the C atom, the bridge site at the middle of the C-C bond of two neighboring C atoms, and the hollow site at the carbon hexagonal center. Results for single Si atom adsorption on graphene are shown [Table 1](#) and [Fig. 2](#). We found out that the silicon atom finally lies to the bridge site on the surface wherever the initial location is (see [Fig. 2b](#)). That means the bridge site is the most stable site for the Si atom adsorbed on graphene. This is similar to single silicon atom adsorbed on graphite and diamond [47, 48], and single N or O atom adsorbed on graphene [60]. For the most stable

structure, which comes from the top site and the hollow site, the adsorption energy is -1.267 eV. The Si atom height is 2.35 Å, and the distance between the Si atom and its nearest C atom is 2.33 Å. The Si-C distance is much larger than that in SiC bulk, which indicates that the Si atom is mainly physically adsorbed on graphene. This is in contrast to the adsorption of Si atom on graphite surface [48]. We also calculated the adsorption energy of Si atom adsorbed on graphene without considering the vdW interaction, which is -0.763 eV. It is obvious that this value is much higher than that of adsorption energy with considering vdW interaction, which indicates that the dispersion forces play an important role in the interaction between the Si atom and graphene. Mulliken charge analysis clearly indicates that the silicon atom gains charge and the graphene loses charge.

The calculated results for the Si₂ cluster adsorption on graphene are shown in Table 1 and Fig. 3. The initial structures of Si₂ cluster on graphene we considered are mainly the Si₂ cluster perpendicular and paralleling to the graphene surface with different locations. The most stable structure of the Si₂ cluster adsorbed on graphene is shown in Fig. 3a, whose adsorption energy is -1.168 eV. For the most stable adsorption site, the Si₂ cluster is found floating above the graphene layer at about 2.15 Å (the Si atom height), and there is no evidence of formation of chemical bonds between the Si₂ cluster and the graphene. For the most stable structure, we found that the Si₂ cluster parallels to graphene surface, and the graphene has a clear distortion as shown in Fig. 3a. On the contrary, in the third most stable structure, the Si₂ cluster perpendicular to graphene surface, whose adsorption energy is higher by 0.133 eV than the most stable one. Compared with the pure most stable Si₂ cluster, we notice that there is only a minute structural change for Si₂ cluster adsorbed on graphene in parallel. The Si-Si bond length decreases slightly from 2.30 Å in

the isolated Si_2 cluster to 2.29 Å in the case of Si_2 cluster adsorbed on graphene in parallel without respect to where its initial location is. However, when Si_2 cluster vertically adsorbed on graphene, no structural change is found. Considering the charge transfer between cluster and graphene, we found that approximately 0.223 e charge transfers from graphene to the Si_2 cluster in the most stable structure. For the third stable isomer, we found the charge transfer is much smaller with a value of 0.014 e . The found charge transfer is so small that it is doubtful whether it will have any substantial influence on the electronic properties of graphene.

For Si_3 cluster adsorbed on graphene, we considered two isomers of pure Si_3 cluster, which can be considered as the most stable structure because that the energy difference is very small with a value of 0.031 eV (see Fig. 1). We put the two isomers on graphene with perpendicularizing or paralleling to the graphene surface at various locations, so that we can find the most stable structure of Si_3 cluster adsorbed on graphene after optimized. See Fig. 4, the results displayed that the Si_3 cluster plane almost parallels to graphene surface in the lowest-energy structures. For the most stable structure (Fig. 4a), its adsorption energy is -1.277 eV and lower only by 0.036 eV than the second most stable structure (Fig. 4b). In the second stable structures, the Si_3 cluster plane mainly perpendiculars to graphene surface. The cluster-graphene distances are all above 3.2 Å, so that we believe that the Si_3 cluster and the graphene have little chemical interaction. No matter what the initial structures of Si_3 clusters, after adsorption, the Si_3 clusters are all the same structure as shown in Fig. 1 (Si_3 -b).

Considering the relative energy of the second lowest-energy isolated Si_4 isomer is much larger by a value of 1.560 eV than the lowest-energy Si_4 isomer, we just applied the lowest-energy Si_4 cluster on graphene with Si_4 plane perpendicularizing or paralleling to the graphene surface.

Though we had dozens of initial structures, interestingly, the adsorption energies of the optimized geometries are between -1.511 eV and -1.496 eV. Their adsorption energies are quite close, particularly for the structures of the Si_4 plane parallels to the graphene surface, there is only a difference between 0.015 eV. It is worth noting that the lowest-energy structure of Si_4 cluster adsorbed on graphene has four isomers, and the four isomers only have slight structural change as shown in Fig. 5 (a, b, c, and d). Compared with the first four isomers, isomer e and f have so little energy changed that we can consider them as the most stable structure too. This indicates that when the most stable pure Si_4 cluster adsorbed on graphene, it is easy to form the lowest-energy cluster/graphene system with different structures. Resembling the cases of Si_2 and Si_3 clusters adsorbed on graphene, obviously, in all cases considered, the Si_4 cluster was found to maintain its structure, and the Si_4 cluster plane parallels to graphene layer in the most stable Si_4 -cluster/graphene system. This is very similar to the case of Si_4 on graphite surface [48]. The Si_4 cluster is adsorbed above graphene with a distance of about 3.66 Å, which is a little larger than that of Si_4 on graphite surface (3.10~3.30 Å) [48].

Considering that the diversity and complexity of the three-dimensional structures of the lowest-energy isolated Si_5 and Si_6 clusters, it is more difficult for us to find the lowest-energy structures of Si_n -cluster/graphene system. We used three lowest-energy Si_5 and Si_6 isomers (see Fig. 1) adsorbed on graphene with various kinds of initial locations in order to obtain the most stable structure of Si_n -cluster/graphene system.

Results for the Si_5 clusters adsorption on graphene are shown in Table 1 and Fig. 6. We found that, for the lowest-energy structures of Si_5 -cluster/graphene system, the Si_5 clusters are all the same most stable isolated isomer. Interestingly, the Si_5 cluster in the most stable structure (Fig. 6a)

came from the optimized Si_5 -c structure (see Fig. 1), and its adsorption energy has a quite large value by -2.377 eV. Meanwhile, the Si_5 cluster in isomer b and c as shown in Fig. 6 came from optimized Si_5 -b isomer as shown in Fig. 1, their adsorption energies are higher by about 0.033 eV than that of isomer a. Their adsorption energies are much larger than that of other Si_n clusters adsorbed on graphene. We believe that a large number of the adsorption energies come from geometry optimization of the Si_5 clusters. The structure of Si_5 cluster are found to be the most stable one as shown in Fig. 1(6a). That is to say, the structures of isomer 5b and 5c have changed into the most stable one when they are adsorbed on graphene. The structural changes of Si_5 cluster raise the adsorption energies. To demonstrate this point, we also calculated the adsorption energies of the most stable structure of Si_5 clusters adsorbed on graphene. It is found the structure as shown in Fig. 6(a) can be obtained by the most stable structure of Si_5 clusters adsorbed on graphene, and its adsorption energy is -1.363 eV, which is similar to other Si_n clusters adsorbed on graphene.

Results for the Si_6 clusters adsorption on graphene are shown in Table 1 and Fig. 7. Seeing the three isomers we have given in Fig. 7, we found that they have so similar adsorption energies that they all can be considered as the most stable structure, and the Si_6 isomer on graphene is the most stable pure Si_6 cluster, which is in agreement with the trends of Si_n ($n=2-4$) clusters adsorbed on graphene. Their structural differences are only the location and orientation of Si_6 cluster on graphene.

In order to further investigate the three-dimensional silicon cluster adsorbed on graphene, we have also examined the two optimized Si_{10} clusters on the 4×4 graphene sheet and let the system relax. Results for the Si_{10} clusters adsorption on graphene are shown in Table 1 and Fig. 8. See Fig. 1, we found the relative binding energy of Si_{10} -b isomer is higher by 0.494 eV than that of the

most stable Si_{10} -a isomer. However, for the lowest-energy Si_{10} -cluster/graphene system, the Si_{10} cluster comes from the second lowest-energy pure Si_{10} isomer as shown in Fig. 8a. The adsorption energy of isomer c is only higher by 0.136 eV comparing with that of the most stable isomer a. Isomer b has similar adsorption energy, in whose the Si_{10} cluster has different location compared with that in isomer a.

The cluster-graphene distance (H) and the nearest-neighbor Si-C distance ($D_{\text{Si-C}}$) of the most stable structures of the cluster-graphene systems are summarized in Table 1 and Fig. 9. The cluster-graphene distances increase with the size of Si_n cluster, which is the same behavior as the nearest-neighbor Si-C distances showing. But there is a big valley for the Si_2 -graphene system, which indicates that the Si_2 cluster has strongly interaction with graphene when the Si_2 plane locates parallel to graphene surface.

After presenting the lowest-energy structures, it is worth to discuss the structural properties of small Si_n ($n=1-6, 10$) clusters adsorbed on graphene. Firstly, we considered the impact on Si_n ($n=1-6$) clusters, the small silicon clusters keep as the most stable state as they are free and isolated. Meanwhile, after optimized, some lowest-energy structures of Si_n clusters on graphene are translated into the most stable states. It is a fact of great importance that it will influence many properties and applications of the deposited clusters. However, in contrast to the cases of Si_n ($n=1-6$) clusters, for Si_{10} clusters, the second stable isolated cluster adsorbed on graphene is the most stable. Secondly, considering the impact on the graphene structure, we found that the Si_n clusters adsorbed on graphene basically do not cause changes in the graphene structures. However, for single and two silicon atoms adsorbed on graphene in parallel, there are some obvious distortions on graphene. The C atoms in graphene, which are located near the Si atoms, have a

slight protuberance toward the silicon clusters (see Fig. 1 and Fig. 2a or 2b). This indicates that when single and dimer silicon atoms adsorbed on graphene, the Si atoms and their nearest C atoms have a strong interaction. Thirdly, considering the lowest-energy structures of Si_n -clusters/graphene systems, for each species, the adsorption energy variation between different locations is extremely small, and the strong adsorptions can be obtained from different initial structures. For single Si atom adsorbed on graphene, the Si atom prefers to locate at the bridge site, while the Si_n ($n=2-4$) cluster-planes favor paralleling to graphene surface, which is similar to the cases of Si_n ($n=2-4$) clusters adsorbed on graphite surface [47, 48]. The strong adsorptions of Si_n from n equals 4 adsorbed on graphene become diversified to describe the structural features. As mentioned above, the most stable structures of them in gas phase have isomers, but the silicon clusters always keep the lowest-energy structures as cluster in gas phase. It is noting that the case of the Si_{10} cluster adsorbed on graphene, the strong adsorption can also be obtained from the second lowest-energy structure of isolated Si_{10} cluster on graphene. Finally, it should be noted that the silicon clusters are physisorbed on graphene, which indicates that the interaction between them is weak. In such a case, vdW interaction would play an important role. From Table 1, it is found that the adsorption energies with considering vdW interaction are much larger than those without considering vdW interaction. Especially for Si_n ($n=2, 3$) clusters adsorbed on graphene, it is obvious that the most stable structures of Si_n ($n=2, 3$) clusters adsorbed on graphene are the Si_n ($n=2, 3$) clusters parallel to the graphene surface when it is refer to the vdW interaction. Furthermore, we calculate the energy barriers for the migration processes of the two most stable configurations for each size Si_n ($n=1-6, 10$) cluster on graphene, except for the size $n=4$, for which we consider the migration process of configuration e to a as shown in Fig. 5. For Si_n ($n=2, 3, 5, 6$,

10) cluster-graphene complexes, we practically consider the energy barriers of the Si cluster migrates from the site of the second stable configuration to the most stable site, which are listed in Table 1. It can be seen from Table 1 that the migration energy barriers for each size Si_n ($n=2-6, 10$) cluster on graphene are no more than 0.213 eV. Specially, for the size $n=3-6$, the migration energy barriers are no more than 0.1 eV. Therefore, we predict that the mobility of small silicon clusters on graphene will be high at room temperature. It is well known the migration of cluster will limit its applications. However, because of the special structural and electronic properties of the silicon cluster-graphene complex, it is possible to control the properties of silicon cluster-graphene complex via careful preparation seems within grasp, which is very similar to the cases of molecules adsorbed on graphene [21-23].

3.2 Electronic properties of Si_n ($n=1-6, 10$) clusters adsorbed on graphene

Using the Mulliken population analysis method, we calculated the charge transfer between the Si_n cluster and the graphene, the results are summarized in Table 1. Taken as a whole, there is a charge transfer from graphene to Si_n clusters. The found charge transfers in the stable Si-graphene and Si_2 -graphene systems are above 0.20 e. This indicates that the single and dimer Si atoms have a relative strong ionic bonding with the graphene, and it is no doubt that these will have substantial influence on the electronic properties of graphene. From the species of the Si_3 cluster-graphene system, we found that the differences for the charge transfer between different configurations are within 0.005 e, which shows that in each species the charge transfer does not highly depend on the adsorption position with the cluster size increasing from 3. Meanwhile, the charge transfer according to Mulliken population analysis are quite small, which may have little influence on the electronic properties of graphene.

In order to investigate the detailed electronic structures of the Si_n -cluster/graphene system, we have calculated the band structures of the most stable structures of Si_n -cluster/graphene system. The band gaps are potted in [Table 1](#). Our calculations show that the Si_n -cluster/graphene systems are semiconductors with energy gap, which increases as a function of cluster size. However when the cluster size increase to five, the energy gap remains unchanged (1.17 eV). It is well known that the pristine graphene has a unique electronic structure with a zero gap. For its applications to electrical and optical devices, it is important to control the band gap. Our calculations illustrate that the adsorption of Si_n cluster will be an effective method for opening of an energy gap. Especially, the adsorption of Si_n cluster with large size ($n \geq 5$) would have a band gap with a larger and constant energy value.

Furthermore, we also calculate the total and partial density of states (PDOS) for the most stable structures of Si_n -cluster/graphene system. The results are shown in [Fig. 10](#). It is found that the PDOS of all structures exhibit similar features, which could be tracked back to the atomic valences states: C 2s and 2p and Si 3s and 3p. The valence bands near Fermi level are mainly dominated by the 3p atomic orbitals of Si atoms, and the contribution of the other atomic orbitals to the valence bands is very small. It is clear that the DOS at the Fermi level mainly originates from the adsorbed clusters (e.g. see [Fig. 10](#)(Si1-G, Si2-G, and Si4-G)), which is the manifestation of cluster-graphene interactions. In fact, the graphene in the cluster-graphene complex contributes only a little to the overall DOS at Fermi energy. The calculated DOS of graphene in the presence of the Si_n clusters clearly show discrete molecular levels around the Fermi energy. The presence of flat molecular levels of Si_n clusters in cluster-graphene systems at slightly above the Fermi level, gives rise to significant DOS within the band gap.

4. Conclusions

The adsorption of small Si_n clusters ($n=1-6, 10$) on graphene are studied by use of density functional theory within periodic boundary conditions. The results show that the structural and electronic properties of the deposited Si_n clusters are weakly affected by their interaction with the graphene, however, it is noted that some lowest-energy structures of Si_n clusters are translated into the most stable states by their interaction with the graphene. This indicates that though the Si_n clusters have kinds of configurations within different energy in gas phase, they would be reached the most stable one on graphene substrate. The adsorption energy difference of different adsorption sites for the same size Si cluster on graphene is very small, indicating the Si_n -cluster/graphene system will be obtained easily. There is a little charge transfer from Si_n clusters to graphene when the cluster size is large. The adsorption of Si_n clusters will be an effective method to open of an energy gap for graphene, which is useful for the applications of graphene to electrical and optical devices. Especially, the adsorption of Si_n cluster with large size ($n \geq 5$) would have a band gap with larger and constant energy value.

Acknowledgements

This work was supported by the National Natural Science Foundation of China (No. 11304080 and No. 51302065).

References

1. P. J. Feibelman, *Phys. Rev. Lett.* 1987, **58**, 2766–2769.
2. Y. Tai, W. Yamaguchi, Y. Maruyama, K. Yoshimura and J. Murakami, *J. Chem. Phys.* 2000, **113**, 3808–3813.
3. L. Motte, E. Lacaze, M. Maillard and M. P. Pileni, *Langmuir* 2000, **16**, 3803–3812.
4. P. M. Voyles, D. A. Muller, J. L. Grazul, P. H. Citrin and H. J. L. Gossmann, *Nature* 2002, **416**,

826–829.

5. A. Pinchuk, A. Hilger, G. von Plessen and U. Kreibitz, *Nanotechnology* 2004, **15**, 1890–1896.
6. F. Fehrer, P. M. Dinh, E. Suraud and P.-G. Reinhard, *Phys. Rev. B* 2007, **75**, 235418 .
7. H. J. Freund, M. Bäumer and H. Kuhlenbeck, *Adv. Catal.* 2000, **45**, 333–384 (2000).
8. *Nanocatalysis*, edited by U. Heiz and U. Landman (Springer, Berlin, 2006).
9. W. E. Kaden, T. Wu, W. A. Kunkel and S. L. Anderson, *Science* 2009, **326**, 826–829.
10. K. S. Novoselov, A. K. Geim, S. V. Morozov, D. Jiang, Y. Zhang, S. V. Dubonos, I. V. Grigorieva and A. A. Firsov, *Science* 2004, **306**, 666–669.
11. K. S. Novoselov, A. K. Geim, S. V. Morozov, D. Jiang, M. I. Katsnelson, I. V. Grigorieva, S. V. Dubonos and A. A. Firsov, *Nature* 2005, **438**, 197–200.
12. Y. Zhang, Y. W. Tan, H. L. Stormer and P. Kim, *Nature* 2005, **438**, 201–204.
13. J. S. Wu, W. Pisula and K. Mullen, *Chem. Rev.* 2007, **107**, 718–747.
14. M. Y. Han, B. Ozyilmaz, Y. Zhang and P. Kim, *Phys. Rev. Lett.* 2007, **98**, 206805 .
15. B. Huard, J. A. Sulpizio, N. Stander, K. Todd, B. Yang and D. Goldhaber-Gordon, *Phys. Rev. Lett.* 2007, **98**, 236803.
16. Ç. Ö. Girit, J. C. Meyer, R. Erni, M. D. Rossell, C. Kisielowski, L. Yang, C. -H. Park, M. F. Crommie, M. L. Cohen, S. G. Louie and A. Zettl, *Science* 2009, **323**, 1705–1708.
17. A. H. Castro Neto, F. Guinea, N. M. R. Peres, K. S. Novoselov and A. K. Geim, *Rev. Mod. Phys.* 2009, **81**, 109–162.
18. A. K. Geim and K. S. Novoselov, *Nat. Mater.* 2007, **6**, 183–191.
19. M. I. Katsnelson, *Mater. Today* 2007, **10**, 20–27.
20. I. Zanella, S. Guerini, S. B. Fagan, J. Mendes Filho and A. G. S. Filho, *Phys. Rev. B* 2008, **77**,

073404.

21. J. Berashevich and T. Chakraborty, *Phys. Rev. B* 2009, **80**, 033404.
22. Y. H. Lu, W. Chen, Y. P. Feng, and P. M. He, *J. Phys. Chem. B* 2009, **113**, 2–5.
23. A. K. Manna and S. K. Pati, *Chem. Asian J.* 2009, **4**, 855–860.
24. M. Farjam and H. Rafii-Tabar, *Phys. Rev. B* 2009, **79**, 045417.
25. L. Pisani, B. Montanari and N. M. Harrison, *New J. Phys.* 2008, **10**, 033002.
26. Y. Okamoto, *Chem. Phys. Lett.* 2006, **420**, 382–386.
27. Y. Sanchez-Paisal, D. Sanchez-Portal and A. Ayuela, *Phys. Rev. B* 2009, **80**, 045428.
28. M. Neek-Amal, R. Asgari and M. R. R. Tabar, *Nanotechnology* 2009, **20**, 135602.
29. E. J. Yoo, T. Okata, T. Akita, M. Kohyama, J. Nakamura and I. Honma, *Nano Lett.* 2009, **9**, 2255–2259.
30. I. Zanella, S. B. Fagan, R. Mota and A. Fazzio, *J. Phys. Chem. C* 2008, **112**, 9163–9167.
31. O. Ü. Aktürk and M. Tomak, *Phys. Rev. B* 2009, **80**, 085417.
32. K. Okazaki-Maeda, Y. Morikawa, S. Tanaka and M. Kohyama, *Surf. Sci.* 2010, **604**, 144–154.
33. K. Okazaki-Maeda, S. Yamakawa, Y. Morikawa, T. Akita, S. Tanaka, H. Hyodo and M. Kohyama, *J. Phys.: Conf. Ser.* 2008, **100**, 072044.
34. O. Leenaerts, B. Partoens and F. M. Peeters, *Phys. Rev. B* 2009, **79**, 235440.
35. K. Raghavachari, *J. Chem. Phys.* 1986, **84**, 5672–5686.
36. K.-M. Ho, A. A. Shvartsburg, B. Pan, Z.-Y. Lu, C.-Z. Wang, J. G. Wacker, J. L. Fye and M. F. Jarrold, *Nature* 1998, **392**, 582–585.
37. C. Pouchan, D. Bégué and D. Y. Zhang, *J. Chem. Phys.* 2004, **121**, 4628–4634.
38. S. Yoo and X. C. Zeng, *J. Chem. Phys.* 2005, **123**, 164303.

39. S. Yoo and X. C. Zeng, *J. Chem. Phys.* 2006, **124**, 054304.
40. A. D. Zdetsis, *J. Chem. Phys.* 2007, **127**, 014314.
41. A. D. Zdetsis, *J. Chem. Phys.* 2007, **127**, 244308 .
42. R. L. Zhou and B. C. Pan, *Phys.Lett. A* 2007, **368**, 396.
43. R. L. Zhou and B. C. Pan, *J. Chem. Phys.* 2008, **128**, 234302.
44. R. L. Zhou and B. C. Pan, *Eur. Phys. J. D* 2008, **47**, 367–372.
45. W. Hellmann, R. G. Hennig, S. Goedecker, C. J. Umrigar, B. Delley and T. Lenosky, *Phys. Rev. B* 2007, **75**, 085411.
46. T. T. Rantala, M. I. Stockman, D. A. Jelski and T. F. George, *J. Chem. Phys.* 1990, **93**, 7427–7438.
47. J. H. Wu, F. Hagelberg and K. Sattler, *Phys. Rev. B* 2005, **72**, 085441.
48. J. H. Wu and F. Hagelberg, *Phys. Rev. B* 2007, **76**, 155409.
49. B. Delley, *J. Chem. Phys.* 1990, **92**, 508–517.
50. B. Delley, *J. Chem. Phys.* 2000, **113**, 7756–7764.
51. J. P. Perdew, K. Burke and M. Ernzerhof, *Phys. Rev. Lett.* 1996, **77**, 3865–3868.
52. A. Tkatchenko and M. Scheffler, *Phys. Rev. Lett.* 2009, **102**, 073005.
53. M. Hassan, M. Walter, and M. Moseler, *Phys. Chem. Chem. Phys.* 2014, **16**, 33–37.
54. J. Åkesson, O. Sundborg, O. Wahlström, and E. Schröder, *J. Chem. Phys.* 2012, **137**, 174702.
55. J. Lee, K. Min, S. Hong, and G. Kim, *Chem. Phys. Lett.* 2012, **618**, 57–62.
56. D. Le, A. Kara, E. Schröder, P. Hyldgaard, and T. S. Rahman, *J. Phys.: Condens. Matter* 2012, **24**, 424210.
57. H. J. Monkhorst and J. D. Pack, *Phys. Rev. B* 1976, **13**, 5188–5192.

58. T. A. Halgren and W. N. Lipscomb, *Chem. Phys. Lett.* 1977, **49**, 225–232.
59. G. Henkelman and H. Jónsson, *J. Chem. Phys.* 2000, **113**, 9978–9985.
60. M. Wu, En-Zuo Liu and J. Z. Jiang, *Appl. Phys. Lett.* 2008, **93**, 082504.

Table 1 Calculated results for the Si_n ($n=1-6, 10$) clusters on graphene: the adsorption energies (E_{a-D} : which is calculated with considering the vdW interaction; E_a : which is calculated without considering the vdW interaction); the nearest-neighbor Si-C distances ($D_{\text{Si-C}}$); the cluster height (H), the charge transfer (Δq) from Si_n clusters to graphene, the bandgap energy (E_g), and the migration energy barrier (E_m).

system ^a	E_{a-D} (eV)	E_a (eV)	$D_{\text{Si-C}}$ (Å)	H (Å)	Δq (e)	E_g (eV)	E_m (eV)
Si-G	-1.267	-0.763	2.35	2.33	0.201	0.260	
Si ₂ -G(a)	-1.168	-0.378	2.27	2.15	0.223	0.960	0.213
Si ₂ -G(c)	-1.037	-0.508	4.08	3.84	0.014		
Si ₃ -G(a)	-1.277	-0.518	3.29	3.30	0.046	1.260	0.051
Si ₃ -G(b)	-1.205	-0.546	3.65	3.56	0.015		
Si ₄ -G(a)	-1.511	-0.579	3.68	3.66	0.007	1.060	0.041
Si ₅ -G(a)	-2.377	-1.658	3.70	3.70	0.016	1.170	0.073
Si ₅ -G(b)	-2.344	-1.557	3.76	3.76	0.019		
Si ₆ -G(a)	-1.425	-0.550	3.74	3.74	0.019	1.170	0.076
Si ₆ -G(b)	-1.421	-0.548	3.85	3.81	0.022		
Si ₁₀ -G(a)	-2.007	-0.567	3.86	3.86	0.034	1.170	0.147
Si ₁₀ -G(c)	-1.980	-0.555	3.54	3.53	0.035		

^a Notations: Si_n -G represents Si_n clusters-graphene system, and the a, b, and c in parentheses

represents the structures in the corresponding figures.

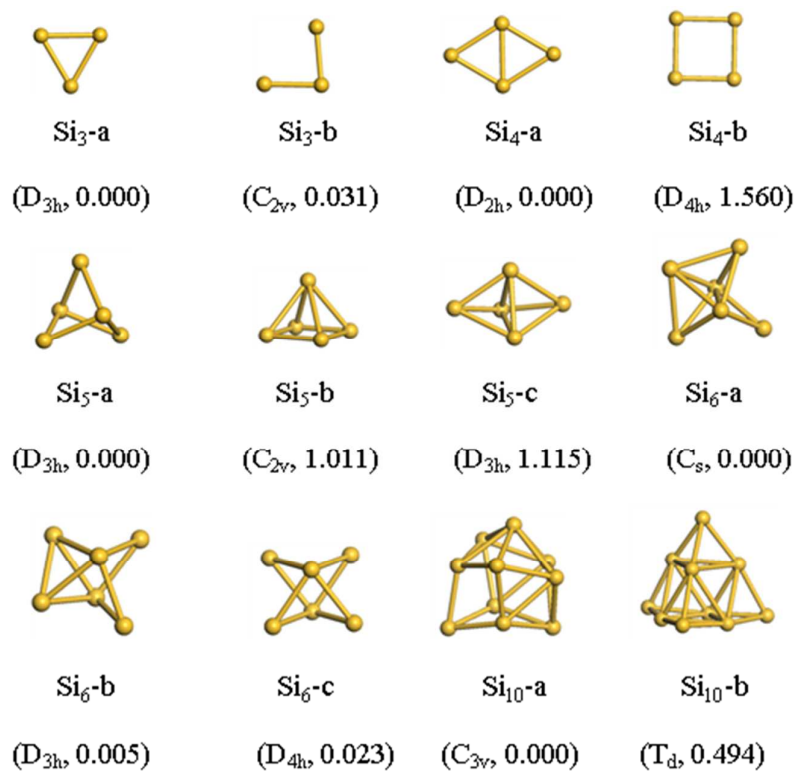


Fig. 1 The lowest-energy structures of Si_n (n=3-6, 10) clusters. Isomeric structures for Si_n clusters are labeled as a, b, and c in order of decreasing stability for each species. Values in parentheses are symmetries and relative energies in eV.

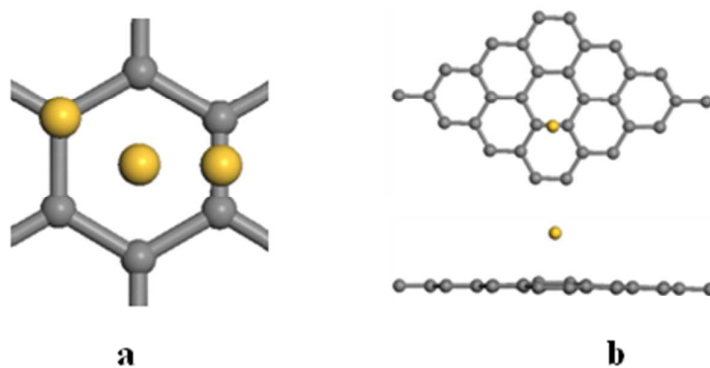


Fig. 2 (a) The three adsorption sites considered for single Si atom on graphene, (b) View of the most stable configuration for the single Si atom adsorption on graphene from the top and the side of the graphene surface. In this and following figures, grey and yellow balls represent C and Si atoms, respectively.

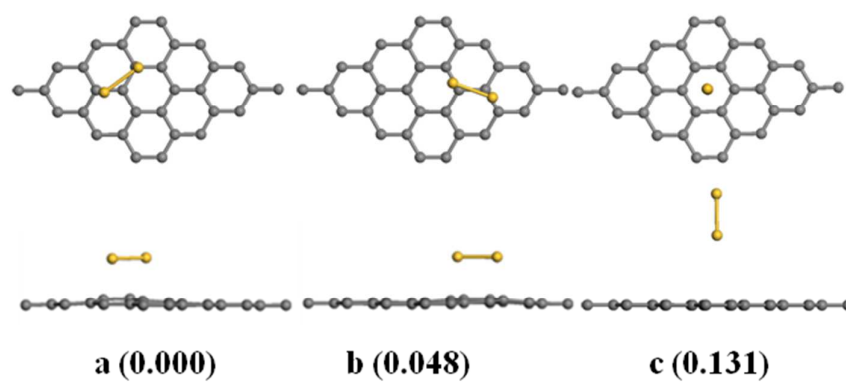


Fig. 3 Stable configurations for the Si_2 clusters adsorption on graphene. Schematic views from the top and the side of the graphene surface. Isomeric structures are labeled as a, b, and c in order of decreasing stability. Values in parentheses are relative energies in eV, which are obtained by DFT-D method.

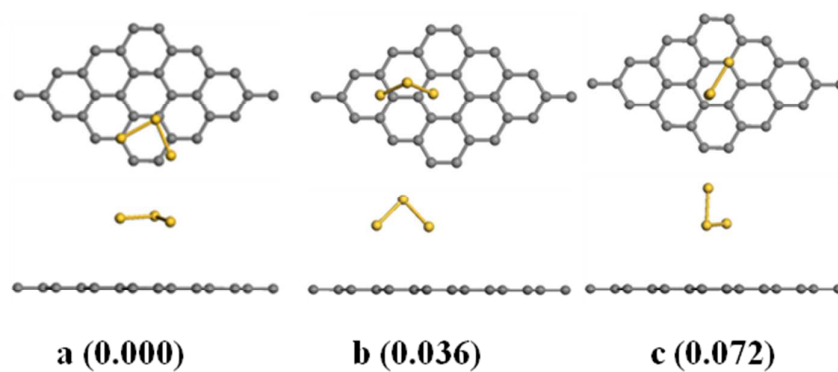


Fig. 4 Stable configurations for the Si_3 clusters adsorption on graphene. Schematic views from the top and the side of the graphene surface. Isomeric structures are labeled as a, b, and c in order of decreasing stability. Values in parentheses are relative energies in eV, which are obtained by DFT-D method.

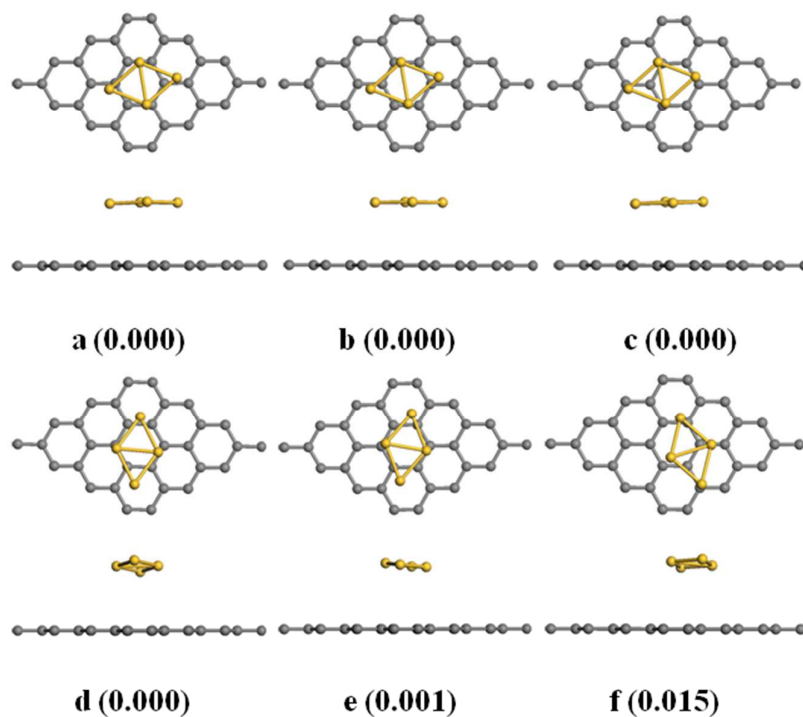


Fig. 5 Stable configurations for the Si_4 clusters adsorption on graphene. Schematic views from the top and the side of the graphene surface. Isomeric structures are labeled as a, b, c, etc., in order of decreasing stability. Values in parentheses are relative energies in eV, which are obtained by DFT-D method.

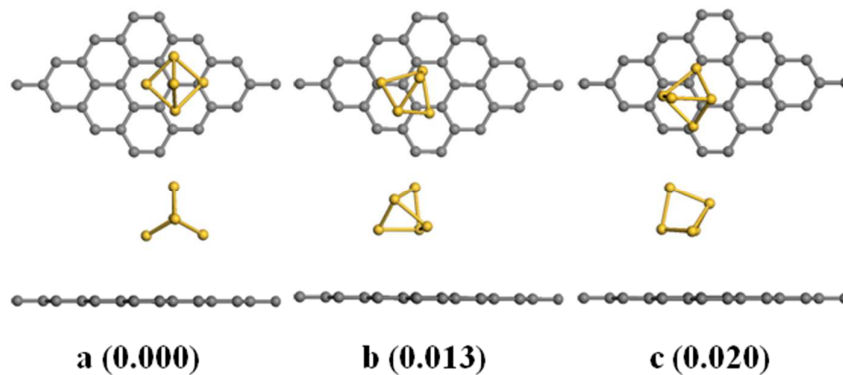


Fig. 6 Stable configurations for the Si₅ clusters adsorption on graphene. Schematic views from the top and the side of the graphene surface. Isomeric structures are labeled as a, b, and c in order of decreasing stability. Values in parentheses are relative energies in eV, which are obtained by DFT-D method.

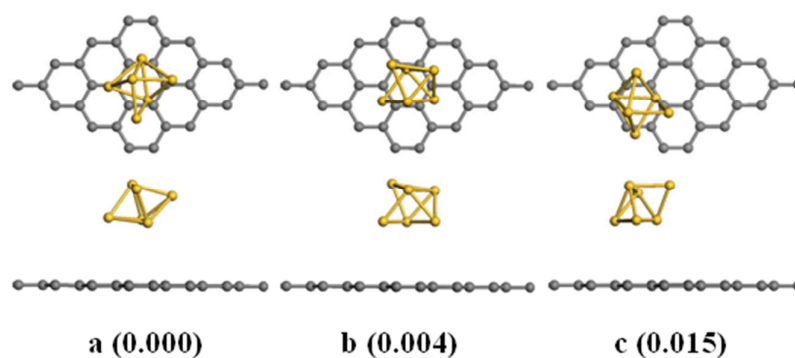


Fig. 7 Stable configurations for the Si₆ clusters adsorption on graphene. Schematic views from the top and the side of the graphene surface. Isomeric structures are labeled as a, b, and c in order of decreasing stability. Values in parentheses are relative energies in eV, which are obtained by DFT-D method.

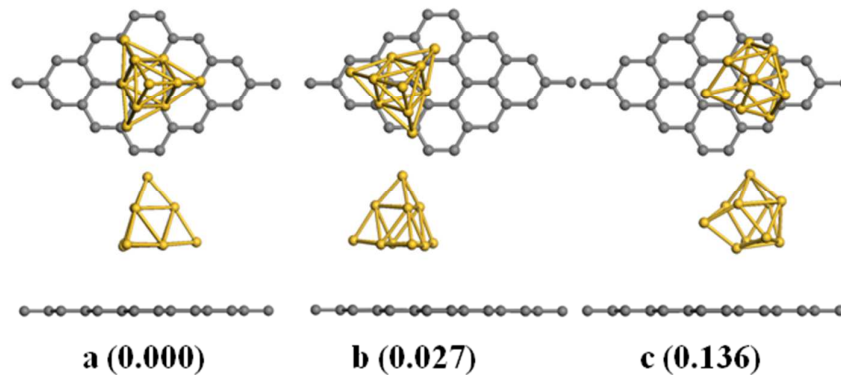


Fig. 8 Stable configurations for the Si₁₀ clusters adsorption on graphene. Schematic views from the top and the side of the graphene surface. Isomeric structures are labeled as a, b, and c in order of decreasing stability. Values in parentheses are relative energies in eV, which are obtained by DFT-D method.

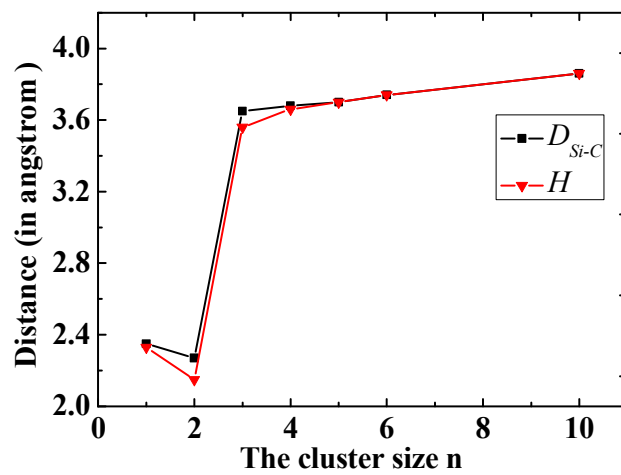


Fig. 9 The cluster-graphene distance (H) and the nearest-neighbor Si-C distance (D_{Si-C}) for the most stable structures of the cluster-graphene systems as a function of the cluster size n .

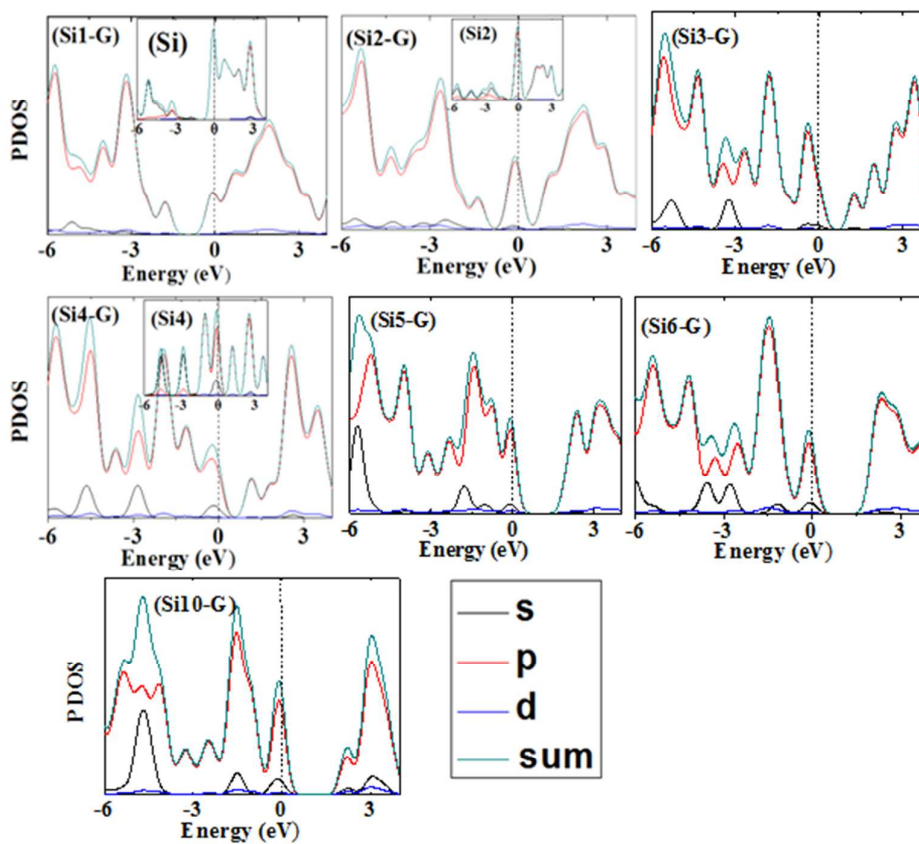


Fig. 10 Total and partial density of states (PDOS) of the most stable structures for the Si_n ($n=1-6, 10$) clusters adsorbed on graphene. The vertical line indicates the Fermi level. $\text{Si}_n\text{-G}$ ($n=1-6, 10$) represents the Si_n ($n=1-6, 10$) clusters adsorbed on graphene. The interpolated figures in figures Si1-G, Si2-G, and Si4-G represent the PDOS of the corresponding clusters.